JOURNAL OF GEOPHYSICAL RESEARCH, VOL. 113, A07204, doi:10.1029/2008JA013178, 2008

Statistical properties of the multiple ion band structures observed by the FAST satellite

Y. Yao,[1] K. Seki,[1,2] Y. Miyoshi,[1] J. P. McFadden,[3] E. J. Lund,[4] and C. W. Carlson[3]

Received 18 March 2008; revised 6 May 2008; accepted 15 May 2008; published 4 July 2008.

[1] Data of low-energy (<28 keV) H^+ and O^+ ions obtained by the FAST satellite were used to investigate the statistical properties of multiple ion band structures (MIBS) that are characterized by multiple O^+/H^+ components with discrete energies. MIBS distributions for H^+ and O^+ ions had different relationships with the *AL* index, invariant latitude (ILAT), and magnetic local time, suggesting different formation mechanisms. O^+ MIBSs were observed during magnetically active periods around the equatorward boundary of the auroral oval mainly in the dusk and midnight sectors, while H^+ MIBSs were observed during quiet times at higher latitudes in the dawn and dusk sectors. O^+ MIBSs shifted toward lower latitudes with decreasing *AL* index due to the expansion of the auroral oval during magnetically active periods. Both maximum and minimum energies of O^+ MIBSs decrease with decreasing ILAT, which is consistent with velocity filter effects caused by convective transport from high to low latitudes in the nightside. The statistical properties obtained from the FAST observations suggest that O^+ MIBSs supply O^+ ions from the ionosphere to the inner magnetosphere during magnetic storms and contribute to the storm time ring current development.

Citation: Yao, Y., K. Seki, Y. Miyoshi, J. P. McFadden, E. J. Lund, and C. W. Carlson (2008), Statistical properties of the multiple ion band structures observed by the FAST satellite, *J. Geophys. Res.*, *113*, A07204, doi:10.1029/2008JA013178.

1. Introduction

[2] The multiple ion band structure (MIBS), which is characterized by an ion energy distribution with multiple ion components at discrete energies, has been observed by many satellites, such as DE [e.g., *Winningham et al.*, 1984], Akebono [e.g., *Hirahara et al.*, 1996, 1997], FAST [e.g., *McFadden et al.*, 2003], Cluster [e.g., *Keiling et al.*, 2004], Interball-Auroral [e.g., *Sauvaud and Kovrazhkin*, 2004], and Geotail [e.g., *Seki et al.*, 1999; *Hirahara et al.*, 2000]. Two models have been proposed to interpret the energy dispersion of MIBSs in the ion energy-time spectrogram [e.g., *Frahm et al.*, 1986]. The first is caused by combination of the finite duration of the source and the time-of-flight (TOF) effect [*Quinn and McIlwain*, 1979], which explained certain features of bouncing ions observed in geosynchronous orbit. The second is the TOF with convection effect discussed by *Winningham et al.* [1984], which explained how upflowing ions from opposite hemisphere produce the dispersed ion bands. *Hirahara et al.* [1996] investigated the differences in the ion compositions of MIBSs and identified two types of MIBSs using the Akebono observations. Type I is produced by multiple bouncing H^+ ions originating in the magnetosphere, and Type II is formed by upward flowing ions (UFIs) originating in the ionosphere (mainly O^+ ions).

[3] Past observations have shown that the main ion composition of the ring current changes from H^+ to O^+ during intense magnetic storms [e.g., *Daglis et al.*, 1999]. However, the close connection of enhanced O^+ outflows from the ionosphere to the O^+ ring current during magnetically active periods [e.g., *Yau and André*, 1997] is poorly understood. *Seki et al.* [2005] reported a MIBS event in the region of invariant latitude (ILAT) = 50°–60° recorded by FAST. This event involved the coexistence of multiple O^+ components at discrete energies up to several keV bouncing along the local magnetic field line during the April 2001 magnetic storm. On the basis of the energy ratio of each band and results of the trajectory tracing using empirical magnetic and electric field models, they concluded that the O^+ ions are UFIs from the ionosphere, and their ejection coincides roughly with the interplanetary shock arrival. *Seki et al.* [2005] also showed their possible contribution to the storm time O^+ ring current. Their study was based on one event, and the statistical properties of these multiple ion band structures are not known. In the present study, a statistical analysis was carried out on both H^+ and O^+ MIBSs. The FAST observations were used to investigate

[1]Solar-Terrestrial Environment Laboratory, Nagoya University, Nagoya, Japan.
[2]Also at Institute for Advanced Research, Nagoya University, Nagoya, Japan.
[3]Space Sciences Laboratory, University of California, Berkeley, California, USA.
[4]Space Science Center, University of New Hampshire, Durham, New Hampshire, USA.

0148-0227/08/2008JA013178$09.00

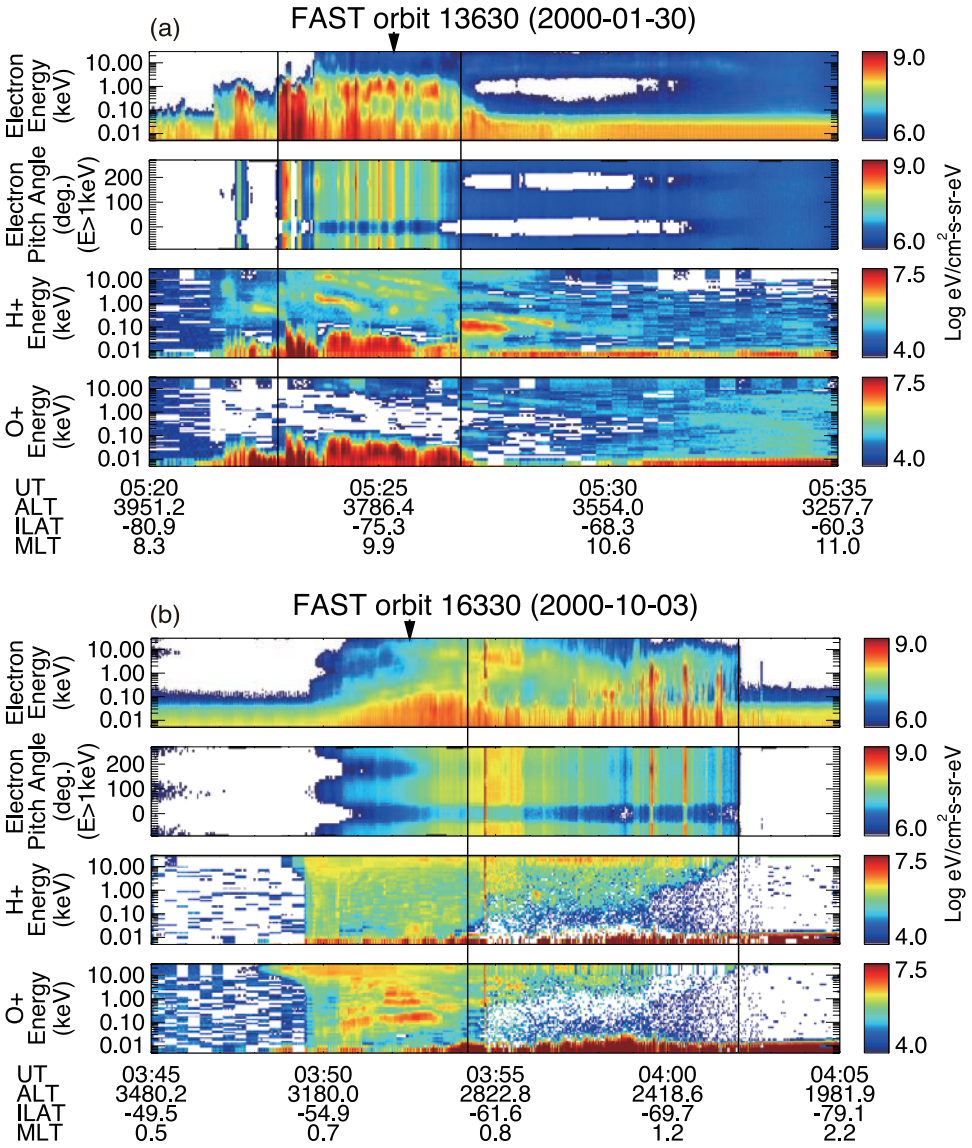

Figure 1. Examples of the multiple ion band structures (MIBS) events for (a) H^+ ions (orbit 13630) and (b) O^+ ions (orbit 16330). From top to bottom, the four panels of Figures 1a and 1b show the energy-time (E-t) spectrogram of electrons, pitch angle distribution of electrons with energies >1 keV, E-t spectrogram of H^+ ions, and the E-t spectrogram of O^+ ions. The white areas in the spectrograms denote energy flux below the color bar.

their dependence on magnetic local time (MLT), ILAT, and geomagnetic activities.

2. Instrumentation and Data Sets

[4] Data for this study were obtained using the Electrostatic Analyzer (ESA) [*Carlson et al.*, 2001] and the Time-of-flight Energy Angle Mass Spectrograph (TEAMS) [*Klumpar et al.*, 2001] onboard the FAST satellite. The ESA measures electrons from 4 eV to 30 keV and ions from 3 eV to 28 keV. The TEAMS instrument is a mass-resolving ion spectrometer designed to measure the full three-dimensional distribution functions of major ion species (including H^+, He^+, He^{++} and O^+) in the lower energy range (up to 12 keV). However, the pitch angle distribution data are not available from TEAMS during the period used in this study. The energy flux ratio of each ion species provided from TEAMS as a function of energy is multiplied by the ESA data to obtain the two-dimensional pitch angle distributions of O^+ and H^+ ions. Composition of ions with energy from 12 keV to 28 keV was determined by extrapolation. The particle data at middle latitudes are generally contaminated by radiation belt electrons. In this study, the automated noise correction method was used, which subtracted the high-energy electron noise from the original data using the count rate in the loss cone [*Seki et al.*, 2005; *Yao et al.*, 2008]. The combination of ESA and TEAMS used in this study makes it possible to observe fast time variation of ions at subauroral latitudes.

[5] A total of 3529 passes of FAST data were available in 2000, covering ILAT from 90° to ~45° and all MLT. The passes in the southern hemisphere cover the MLT range

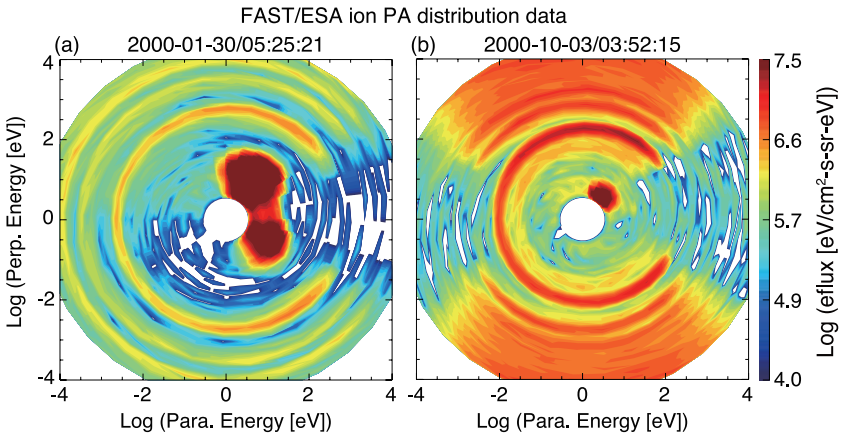

Figure 2. Pitch angle distribution of ESA energy flux. (a) and (b) The distribution data during MIBS events for H^+ and O^+ ions in Figure 1, respectively. Figure 2a corresponds to 0525:21 UT, 30 January, and Figure 2b to 0352:15 UT, 3 October 2000 indicated by solid triangles in Figure 1. In Figures 2a and 2b, the vertical (horizontal) axis represents the perpendicular (parallel) direction to the local magnetic field.

from 12 to 03 and ILAT from −60° to −45°. All available passes were surveyed visually and MIBS events were selected based on the following three criteria: (1) the presence of more than two ion bands that overlap temporally, (2) the similarity of the energy variation of each ion component (band) to other bands, and (3) the peak energy flux of each ion band being larger than $10^{5.5}$ (eV/cm^2 s sr eV). As a result, 62 MIBS events of H^+ ions and 89 events of O^+ ions were identified.

3. Observations

[6] Two examples of the MIBS observed by FAST are presented in Figure 1. The H^+ MIBS event shown in Figure 1a was observed on 30 January 2000 from 0523 to 0526 UT during a magnetically quiet period. Three H^+ bands can be clearly seen during the time interval in a high ILAT region (around −75°) around 10 MLT. Several inverted-V structures in electron precipitation (Figure 1a, top) were observed during this event, indicating that the H^+ MIBS occurred inside the auroral oval. Intense H^+ distribution in the energy range from 10 to 100 eV in the third panel of Figure 1a shows a typical pitch angle distribution of ion conics (not shown).

[7] The O^+ MIBS event shown in Figure 1b was observed on 3 October 2000 from 0351 to 0354 UT during a magnetically active period, when the *Dst* and *Kp* indices were −47 nT and 5-, respectively. Three O^+ bands can also be clearly seen in this event. The O^+ MIBS was located in a low-latitude region from −57° to −59° in the midnight sector (0.7–0.8 MLT), which corresponds to the transition region from double to single loss cone pitch angle distributions. The two vertical black lines in Figures 1a and 1b denote the equatorward and poleward boundaries of the auroral oval for each MIBS event. We identified the equatorward boundary of the auroral oval by the transition latitude from single to double loss cone distributions in the high-energy (>1 keV) electron observations [*Andersson et al.*, 2004]. The poleward boundary of the auroral oval was identified by the poleward edge of the inverted-V shaped electron precipitation.

[8] Figure 2 shows the pitch angle distributions obtained with ESA instrument during two MIBS examples shown in Figure 1. Figure 2a and 2b correspond to the H^+ and O^+ MIBS events shown in the Figure 1, respectively. In Figure 2a, the pitch angle distribution of H^+ ions shows a single loss cone distribution. The H^+ ions were observed in quiet time around 9.9 MLT. In Figure 2b, the pitch angle distribution of O^+ ions shows a different distribution from that of the H^+ ions during magnetic activity. The band with the lowest energy has a single loss cone distribution, and other bands have double loss cone distributions, which is consistent with trapped ions bouncing along the magnetic field lines [*Hirahara et al.*, 1997].

[9] The ILAT-MLT diagram in Figure 3 shows that the H^+ (light blue) and O^+ (magenta) MIBS events have very different spatial distributions. The O^+ events are mainly seen at lower ILAT (around 60°) and from the dusk (18 MLT) to postmidnight (03 MLT) sectors. In contrast, the H^+ events are mainly distributed in the higher ILAT region (from 70° to 80°) from dawn (06 MLT) to prenoon (11 MLT) and some in the dusk sector. The MLT distribution of H^+ MIBSs has a bite out in the nightside, which may be due to a selection effect as discussed in section 4. The energy range of MIBS events is approximately from 20 eV to 15 keV.

[10] Another important feature is the relationship between magnetic activity and the latitudinal distribution of the MIBSs. Figure 4 illustrates that the latitudinal distribution of the O^+ events exhibit a clear correlation with the *AL* index, that is, the ILAT decreases with decreasing *AL* index. The similar tendency is seen in the relation between the Solar Zenith Angle (SZA) and the *AL* index, though the tendency is less clear (not shown). The result on the SZA suggests that difference between dayside and nightside events is not the dominant factor to create the dependence. Most of the H^+ MIBS events, which are seen mainly at higher latitudes, have single loss cone pitch angle distributions, while many O^+ events, especially at lower latitudes, have double loss cone distributions (Figure 4a, colored error bars). This difference is due to the different locations of H^+

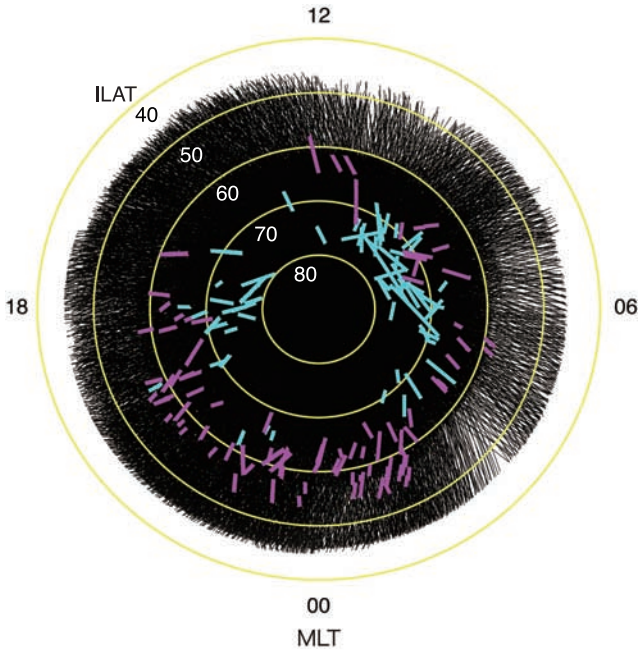

Figure 3. Distribution of the MIBS events in a MLT-ILAT polar diagram. The yellow circles show ILAT lines from 40° to 80° every 10°. Each thick, light blue or magenta line indicates the location of one H^+ or O^+ MIBS event along a part of each FAST pass. The thin black lines represent all available FAST observations.

and O^+ events in the auroral oval. Figure 4b shows the location of the MIBS events relative to the poleward and equatorward boundaries of the aurora oval. The open and solid blue circles are distributed above and below the zero-level ($d\lambda = 0$) horizontal line, respectively. This indicates that the H^+ events were located between the poleward and equatorward boundaries of the auroral oval. The solid red circles are distributed around the horizontal line, which shows that the O^+ MIBS events were mostly observed near the equatorward boundary of the auroral oval. These results also demonstrate that the relative position from the equatorward boundary of the auroral oval does not change with the *AL* index. It is noted that the locations of the O^+ MIBSs show a correlation with the *SYM-H* index; greater negative *SYM-H* values correlated with lower ILAT. Two-thirds (67%) of O^+ MIBSs were observed during the storm time, and 62% of these events occurred in the main phase. We also investigated the dependence of MIBS event location on the solar wind parameters such as the IMF Bz and found that the dependence is less clear compared with that on *AL* and *SYM-H* indices.

[11] The variation in the minimum and maximum energies of O^+ MIBSs with ILAT is shown in Figure 5, together with the total observation time and observational probability in each latitudinal range. The minimum and maximum energies are defined as the smallest and largest energies recorded for each MIBS event and distributed to correspondent latitude bins weighted by observation time in each bin. All O^+ events were divided into two categories, nightside and dayside. The minimum and maximum energies of O^+ MIBSs tended to decrease with decreasing ILAT (Figures 5b and 5d) in the nightside, while there is no clear trend in the dayside events. Although a similar trend can be seen for H^+ events in the dawn side (00–12 of MLT), the tendency is less clear (not shown). The energy decrease with decreasing ILAT for the nightside O^+ events is consistent with the velocity filter effect on bouncing ions caused by the convective transport from high to low latitudes.

4. Summary and Discussion

[12] In this study, we have surveyed FAST data obtained in 2000 during a solar maximum to investigate the statistical properties of multiple ion band structures (MIBSs), which is defined as multicomponent ion energy distribution in which each ion component at discrete energy has similar energy variation in time with other components. The new findings are summarized as follows: (1) H^+ and O^+ MIBSs have different statistical properties. The H^+ MIBSs are mainly observed at high latitudes (65°–75° ILAT) in dawn and dusk sectors with single loss cone pitch angle distributions during quiet times. The O^+ MIBSs are observed at lower latitudes (55°–65° ILAT) from dusk to midnight with double loss cone distributions mainly during magnetic storms. (2) The center ILAT of the O^+ events decreases with decreasing *AL* and *SYM-H* indices. The O^+ MIBSs are seen around the equatorward boundary of the auroral oval regardless of magnetic activity levels. The locations of the

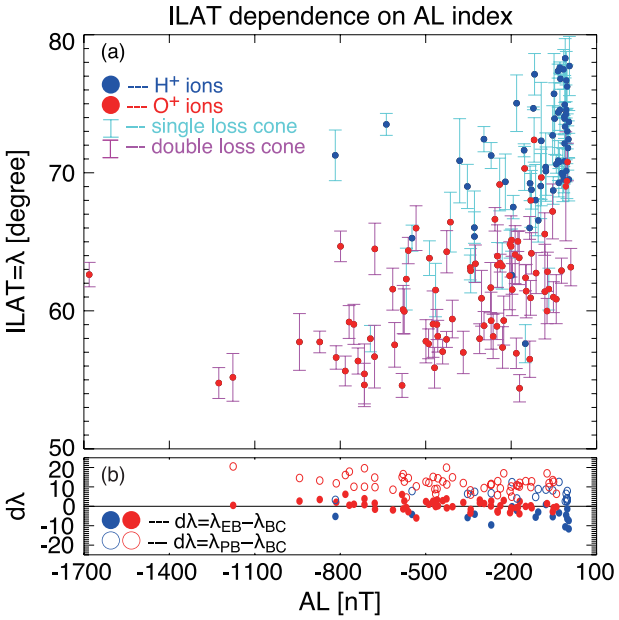

Figure 4. (a) Latitude distribution of the MIBS events as a function of the *AL* index. Blue and red solid circles refer to the center ILAT of the MIBS events of H^+ and O^+ MIBS, respectively. Lengths of error bars represent the ILAT range of the observed MIBS, and color indicates single (light blue) or double (magenta) loss cone distributions. (b) Latitudinal difference between the center ILAT of MIBS events and the auroral oval boundaries as a function of the *AL* index. Blue and red colors correspond to H^+ and O^+ events, respectively. Solid (open) circles refer to the difference in ILAT between the equatorward (poleward) boundary of the auroral oval and the MIBS events.

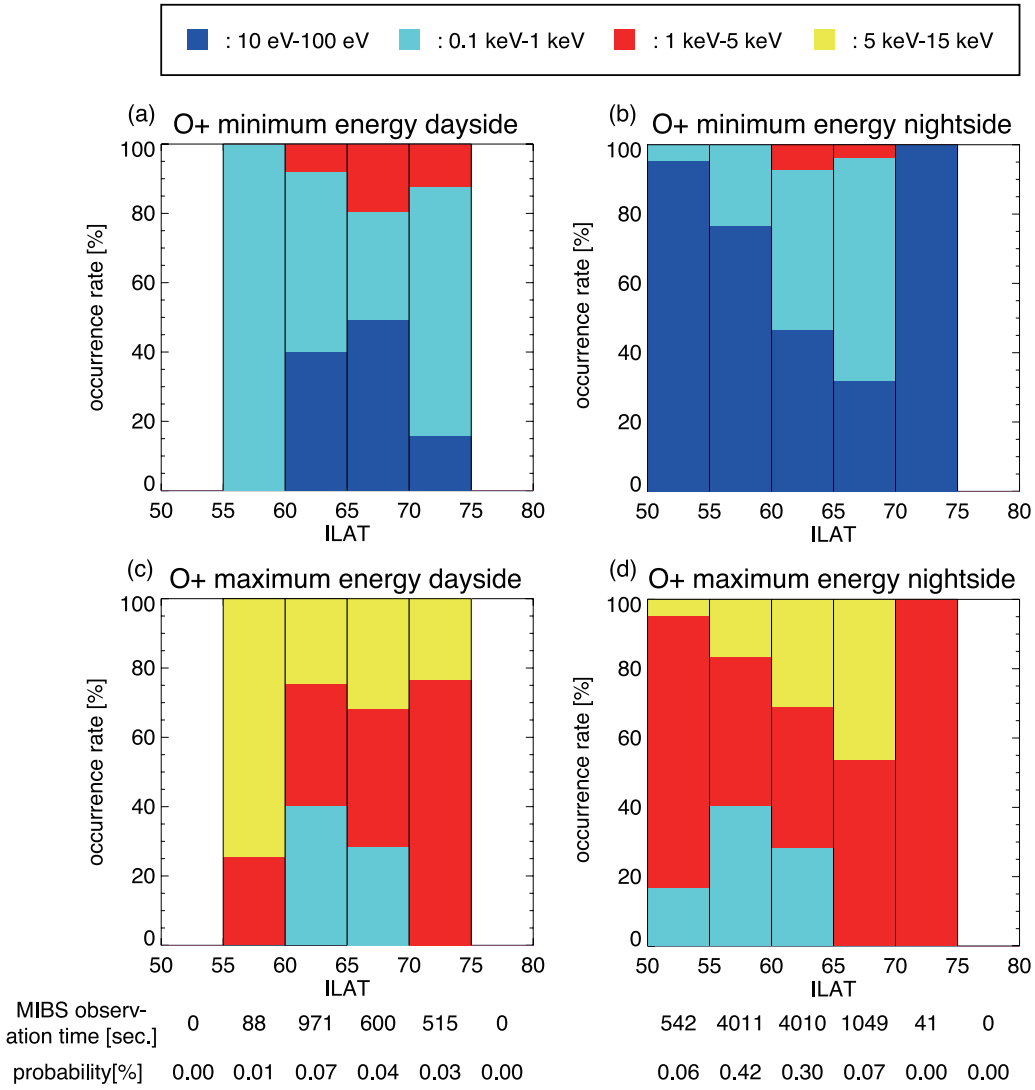

Figure 5. Distributions of (a, b) minimum and (c, d) maximum energies as a function of ILAT for all O^+ MIBS events. Figures 5a and 5c correspond to dayside (06–12 of MLT) events, while Figures 5b and 5d show nightside (12–06 of MLT) events. Minimum and maximum energies are categorized in four ranges distinguished by colors as indicated at the top of the figure. The total observation time and observational probability in each latitude bin are shown at the bottom of the figure.

O^+ MIBSs shift to lower ILAT concurrently with the expansion of the auroral oval when magnetic activity increases. (3) The minimum and maximum energies of the MIBSs decrease with decreasing ILAT, which are clearly seen for O^+ events mainly observed in the nightside. This result is consistent with the velocity filter effects caused by the convective transport.

[13] There are two major candidates for the source of MIBS ions: accelerated plasma sheet ions and UFIs directly from the ionosphere [e.g., *Hirahara et al.*, 1996]. The different pitch angle distributions of the two types of MIBSs indicate that the events occur in different magnetic field geometries. The single loss cone refers to the tail-like magnetic field configuration where pitch angle scattering occurs at the equator, while the double loss cone corresponds to the dipole-like configuration. Both sources are plausible for the H^+ MIBS events observed in the auroral oval. It should be noted that there were many multicomponent H^+ ion signatures whose energy variations were too complex to meet the criteria for this study, particularly in the nightside. Thus, there may be some selection effects due to difficulties in identifying the H^+ MIBSs during magnetic storms, when the band structures are much less clear than those observed during quiet times. The concentration of H^+ MIBS events on the dayside, on the other hand, may indicate that H^+ MIBS events are caused by the pulsed and multiple reconnection sites at the magnetopause [*Boudouridis et al.*, 2002]. For example, the H^+ MIBS shown in Figure 1 was observed during a weak northward IMF period and could have been formed by impulsive particle injection due to pulsed lobe reconnection.

[14] The O^+ MIBSs are a characteristic feature seen primarily during storms. *Hirahara et al.* [1997] showed that dispersed multiple O^+ ion events originate from UFIs at the auroral oval latitudes and are mostly distributed from dusk to midnight. Our statistical results are consistent with

the previous observations. The source of O^+ ions for the storm time ring current is important for the dynamics of magnetic storms [e.g., *Daglis et al.*, 1999]. The previous event study of O^+ MIBSs during the main phase of a storm revealed that the source of O^+ MIBSs is UFIs from the ionosphere whose ejection coincides roughly with the interplanetary shock arrival [*Seki et al.*, 2005]. During magnetic storms, the global convection electric field plays an important role in the plasma transport from high to low latitudes. The convective electric field causes bouncing O^+ ions to drift latitudinally [e.g., *Zelenyi et al.*, 1990], and it contributes to form MIBSs. In a previous study, a rapid circulation of O^+ ions from the ionosphere to the inner plasma sheet was suggested to explain a set of Interball-Auroral observations during the expansion phase of a substorm on 10 October 1997 [*Delcourt et al.*, 1999]. This study showed that most O^+ MIBSs were observed in the vicinity of the equatorward boundary from dusk to nightside and mainly during the storm main phase. On the basis of our results, it is reasonably suggested that MIBS O^+ ions are supplied from the ionosphere to the storm time ring current by the convective transport.

[15] **Acknowledgments.** This work was supported by the 21st Century COE Program of Nagoya University (“Dynamics of the Sun-Earth-Life Interactive System”), Ryugaku Ikuei Scholarship of Daiko Foundation, and a Grant-in-Aid for Scientific Research (Category B, 20340134) of Japan Society for the Promotion of Science. KS thanks the support of a H17 Research 165 Grant by Toyoaki Shogakukai. JPM, EJL, and CWC were supported by NASA grant NAG5-12590.

[16] Wolfgang Baumjohann thanks Dominique Delcourt and another reviewer for their assistance in evaluating this paper.

References

Andersson, L., W. K. Peterson, and K. M. McBryde (2004), Dynamic coordinates for auroral ion outflow, *J. Geophys. Res.*, *109*, A08201, doi:10.1029/2004JA010424.

Boudouridis, A., H. E. Spence, and T. G. Onsager (2002), A new look at the pulsed reconnection model of the dayside magnetopause, *Adv. Space Rev.*, *30*, 2295–2300.

Carlson, C. W., J. P. McFadden, P. Turin, D. W. Curtis, and A. Magoncelli (2001), The Electron and Ion Plasma Experiment for Fast, *Space Sci. Rev.*, *98*, 33–66.

Daglis, I. A., W. Baumjohann, J. Gleiss, S. Orsini, E. T. Sarris, M. Scholer, B. T. Tsurutani, and D. Vassiliadis (1999), Recent advances, open questions and future directions in solar-terrestrial research, *Phys. Chem. Earth, Part C*, *24*, 5–28.

Delcourt, D. C., N. Dubouloz, J.-A. Sauvaud, and M. Malingre (1999), On the origin of sporadic keV ion injections observed by Interball-Auroral during the expansion phase of a substorm, *J. Geophys. Res.*, *104*, 24,929–24,937.

Frahm, R. A., P. H. Reiff, J. D. Winningham, and J. L. Burch (1986), Banded ion morphology - Main and recovery storm phases, in *Ion Acceleration in the Magnetosphere and Ionosphere*, *Geophys. Monogr. Ser.*, vol. 38, edited by T. Chang et al., pp. 98–107, AGU, Washington, D. C.

Hirahara, M., T. Mukai, T. Nagai, N. Kaya, H. Hayakawa, and H. Fukunishi (1996), Two types of ion energy dispersions observed in the nightside auroral regions during geomagnetically disturbed periods, *J. Geophys. Res.*, *101*, 7749–7768.

Hirahara, M., T. Mukai, E. Sagawa, N. Kaya, and H. Hayakawa (1997), Multiple energy-dispersed ion precipitations in the low-latitude auroral oval: Evidence of $\mathbf{E} \times \mathbf{B}$ drift effect and upward flowing ion contribution, *J. Geophys. Res.*, *102*, 2513–2530.

Hirahara, M., T. Mukai, and K. Seki (2000), Outflowing ionospheric ions observed by Geotail and Akebono and their transport in the near-Earth and mid-tail magnetosphere, *Adv. Space Res.*, *25*, 1591–1601.

Keiling, A., et al. (2004), New properties of energy-dispersed ions in the plasma sheet boundary layer observed by Cluster, *J. Geophys. Res.*, *109*, A05215, doi:10.1029/2003JA010277.

Klumpar, D. M., et al. (2001), The time-of-flight energy, angle, mass spectrograph (TEAMS) experiment for FAST, *Space Sci. Rev.*, *98*, 197–219.

McFadden, J. P., C. W. Carlson, R. Strangeway, and E. Moebius (2003), Observations of downgoing velocity dispersed O^+ and He^+ in the cusp during magnetic storms, *Geophys. Res. Lett.*, *30*(18), 1947, doi:10.1029/2003GL017783.

Quinn, J. M., and C. E. McIlwain (1979), Bouncing ion clusters in the earth’s magnetosphere, *J. Geophys. Res.*, *84*, 7365–7370.

Sauvaud, J.-A., and R. A. Kovrazhkin (2004), Two types of energy-dispersed ion structures at the plasma sheet boundary, *J. Geophys. Res.*, *109*, A12213, doi:10.1029/2003JA010333.

Seki, K., M. Hirahara, T. Terasawa, T. Mukai, and S. Kokubun (1999), Properties of He^+ beams observed by Geotail in the lobe/mantle regions: Comparison with O^+ beams, *J. Geophys. Res.*, *104*, 6973–6986.

Seki, K., J. P. McFadden, R. C. Elphic, M. F. Thomsen, G. D. Reeves, Y. Yao, E. J. Lund, J. W. Bonnell, and C. W. Carlson (2005), On variation of outer radiation belt electrons and O^+ ions in the inner magnetosphere during large magnetic storms: FAST observations, *Eos Trans. AGU*, *86*(52), Fall Meet. Suppl., Abstract SA12A-01.

Winningham, J. D., J. L. Burch, and R. A. Frahm (1984), Bands of ions and angular V’s: A conjugate manifestation of ionospheric ion acceleration, *J. Geophys. Res.*, *89*, 1749–1754.

Yao, Y., K. Seki, Y. Miyoshi, J. P. McFadden, E. J. Lund, and C. W. Carlson (2008), Effect of solar wind variation on low-energy O^+ populations in the magnetosphere during geomagnetic storms: FAST observations, *J. Geophys. Res.*, *113*, A04220, doi:10.1029/2007JA012681.

Yau, A. W., and M. André (1997), Sources of ion outflow in the high latitude ionosphere, *Space Sci. Rev.*, *80*, 1–25.

Zelenyi, L. M., R. A. Kovrazkhin, and J. M. Bosqued (1990), Velocity-dispersed ion beams in the nightside auroral zone - AUREOL 3 observations, *J. Geophys. Res.*, *95*, 12,119–12,139.

C. W. Carlson and J. P. McFadden, Space Sciences Laboratory, University of California, Berkeley, CA 94720, USA. (cwc@ssl.berkeley.edu; mcfadden@ssl.berkeley.edu)

E. J. Lund, Space Science Center, University of New Hampshire, Durham, NH 03824, USA. (eric.lund@unh.edu)

Y. Miyoshi, K. Seki, and Y. Yao, Solar-Terrestrial Environment Laboratory, Nagoya University, Nagoya, 464-8601, Japan. (miyoshi@stelab.nagoya-u.ac.jp; seki@stelab.nagoya-u.ac.jp; yaoyao@stelab.nagoya-u.ac.jp)